

Herschel/HIFI search for H_2^{17}O and H_2^{18}O in IRC+10216: constraints on models for the origin of water vapor

David A. Neufeld¹, Volker Tolls², Marcelino Agúndez^{3,4}, Eduardo González-Alfonso⁵,
Leen Decin^{6,7}, Fabien Daniel⁸, José Cernicharo⁸, Gary J. Melnick², Mirosław Schmidt⁹ and
Ryszard Szczerba⁹

ABSTRACT

We report the results of a sensitive search for the minor isotopologues of water, H_2^{17}O and H_2^{18}O , toward the carbon-rich AGB star IRC+10216 (a.k.a. CW Leonis) using the HIFI instrument on the *Herschel Space Observatory*. This search was motivated by the fact that any detection of isotopic enhancement in the H_2^{17}O and H_2^{18}O abundances would have strongly implicated CO photodissociation as the source of the atomic oxygen needed to produce water in a carbon-rich circumstellar envelope. Our observations place an upper limit of 1/470 on the $\text{H}_2^{17}\text{O}/\text{H}_2^{16}\text{O}$ abundance ratio. Given the isotopic $^{17}\text{O}/^{16}\text{O}$ ratio of 1/840 inferred previously for the photosphere of IRC+10216, this result places an upper limit

*Herschel is an ESA space observatory with science instruments provided by European-led Principal Investigator consortia and with important participation from NASA

¹Department of Physics and Astronomy, Johns Hopkins University, 3400 North Charles Street, Baltimore, MD 21218, USA

²Harvard-Smithsonian CfA, 60 Garden Street, Cambridge, MA 02138, USA

³Univ. Bordeaux, LAB, UMR 5804, F-33270, Floirac, France

⁴CNRS, LAB, UMR 5804, F-33270, Floirac, France

⁵Universidad de Alcalá de Henares, Departamento de Física y Matemáticas, Campus Universitario, E-28871 Alcalá de Henares, Madrid, Spain

⁶Instituut voor Sterrenkunde, Katholieke Universiteit Leuven, Celestijnenlaan 200D, 3001 Leuven, Belgium

⁷Sterrenkundig Instituut Anton Pannekoek, University of Amsterdam, Science Park 904, NL-1098 Amsterdam, The Netherlands

⁸Departamento de Astrofísica, Centro de Astrobiología, CSIC-INTA, Ctra. de Torrejón a Ajalvir km 4, 28850, Madrid, Spain

⁹Nicolaus Copernicus Astronomical Center, Polish Academy of Sciences, Rabiańska 8, 87-100, Toruń, Poland

of a factor 1.8 on the extent of any isotope-selective enhancement of H_2^{17}O in the circumstellar material, and provides an important constraint on any model that invokes CO photodissociation as the source of O for H_2O production. In the context of the clumpy photodissociation model proposed previously for the origin of water in IRC+10216, our limit implies that $^{12}\text{C}^{16}\text{O}$ (not $^{13}\text{C}^{16}\text{O}$ or SiO) must be the dominant source of ^{16}O for H_2O production, and that the effects of self-shielding can only have reduced the $^{12}\text{C}^{16}\text{O}$ photodissociation rate by at most a factor ~ 2 .

Subject headings: circumstellar matter — stars: AGB and post-AGB — stars: abundances

1. Introduction

A key *Herschel* result of relevance to evolved stars has been the discovery of water vapor in the warm inner envelope of the carbon-rich AGB star IRC+10216 (a.k.a. CW Leonis). Here, SPIRE, PACS, and HIFI observations of multiple water transitions emitted by the dense outflowing envelope of this star have established (Decin et al. 2010a; Neufeld et al. 2011a) the presence of warm water vapor within a few stellar radii of the stellar photosphere. The presence of water vapor so close to the star definitively rules out a previous suggestion that the origin of the water vapor, originally detected by means of Submillimeter Wave Astronomy Satellite (SWAS) observations of a single water transition (Melnick et al. 2001, Ford & Neufeld 2001), was the vaporization of a Kuiper Belt analog. In addition, and very strikingly, a small HIFI survey for water vapor in eight additional carbon-rich AGB stars has led to the detection of water emission from all eight sources, suggesting that the presence of water in carbon-rich AGB stars is nearly universal (Neufeld et al. 2011b). Moreover, strong similarities in all eight sources between the spectral line profiles of water and those of other species such as CO argue against the water being released from a flattened structure such as a Kuiper Belt analog.

The widespread occurrence of water in these sources is surprising, because the carbon-to-oxygen ratio is the critical determinant of the photospheric chemistry in evolved stars. The photospheres of oxygen rich-stars, with C/O ratios < 1 , are dominated by CO and H_2O ; those of carbon-rich stars, by contrast, are dominated by CO, HCN, and C_2H_2 and – under conditions of thermochemical equilibrium – are expected to contain very little H_2O . The water abundances derived from *Herschel* observations of carbon-rich AGB stars are typically 3 to 4 orders of magnitude larger than the photospheric abundance expected under conditions of thermochemical equilibrium. This huge discrepancy, first revealed in IRC+10216

by SWAS, had led to the suggestion of several possible origins for the water vapor, including (1) the vaporisation of icy objects (comets or dwarf planets) in orbit around the star (Ford & Neufeld 2001); (2) Fischer-Tropsch catalysis (Willacy 2004); (3) photochemistry within an outer, photodissociated shell (Agúndez & Cernicharo 2006); (4) photochemistry within a clumpy outflow (Decin et al. 2010a; Agúndez, Cernicharo & Guélin 2010); (5) non-equilibrium chemistry associated with pulsationally-driven shock waves (Cherchneff 2011, 2012). At least in the case of IRC+10216, the first three of these suggestions can be ruled out by the relative strengths of the many water transitions detected by *Herschel*. Here, the large relative strength of high-lying water transitions indicates the presence of warm water vapor close to the star, whereas the models for origins (1) - (3) predict an absence of abundant water within ~ 100 AU of the star.

Using the Heterodyne Instrument for the Infrared (HIFI; de Graauw et al. 2010) on board the *Herschel Space Observatory* (Pilbratt et al. 2010), we have attempted to distinguish between the remaining origins (4 and 5 above) by means of deep searches for the minor isotopologues H_2^{17}O and H_2^{18}O . Any explanation for the presence of water vapor in a carbon-rich environment must posit the release of oxygen atoms from the strongly-bound CO molecule. If that release results from photodissociation by ultraviolet radiation, an enhancement in the abundances H_2^{17}O and H_2^{18}O might be expected relative to that of H_2^{16}O . This possibility follows from the physics of CO photodissociation, which takes place following *line* absorption to predissociated electronic states. Therefore, once the transitions of relevance become optically-thick, CO can shield itself from photodissociation; thus the photodissociation rate for ^{13}CO , C^{17}O and C^{18}O (per molecule) can significantly exceed that of $^{12}\text{C}^{16}\text{O}$. Similar effects have been proposed, for example, by Lyons & Young (2005) as an explanation for isotopic anomalies in the solar nebula.

This isotope-selective photodissociation of CO preferentially produces ^{17}O and ^{18}O , which will then go on to form the minor isotopologues of water vapor. By contrast, an origin for the water vapor that does *not* involve the photodissociation of CO, as in the shock-driven chemistry model proposed very recently by Cherchneff (2011, 2012), makes the strong prediction that the $\text{H}_2^{17}\text{O}/\text{H}_2^{16}\text{O}$ and $\text{H}_2^{18}\text{O}/\text{H}_2^{16}\text{O}$ ratios should equal the isotopic abundance ratios in the photosphere: $^{17}\text{O}/^{16}\text{O} = 1/840$ and $^{18}\text{O}/^{16}\text{O} \sim 1/1260$ (Kahane et al. 1992)¹ This prediction follows from the fact that gas-phase reactions are unlikely to

¹ These isotopic abundance ratios were determined from single-dish observations of optically-thin transitions of ^{13}CO , C^{17}O , C^{18}O , ^{13}CS , and C^{34}S within the circumstellar outflow, under the assumption that isotopic fractionation and isotope-selective photodissociation are negligible for these minor isotopologues of CO and CS. Kahane et al. (1992) justified that assumption with reference to theoretical models – which suggest that fractionation is only important in the outermost part of the envelope – and by comparing the

provide any significant isotopic fractionation, because the particle kinetic energies at the high temperatures of the inner envelope are much larger than any zero-point energy differences between the relevant molecular isotopologues.

As discussed by Neufeld et al. (2011a), previous data available from a full HIFI spectral scan of IRC+10216 place upper limits of 5×10^{-3} (3σ) on the $\text{H}_2^{17}\text{O}/\text{H}_2^{16}\text{O}$ and $\text{H}_2^{18}\text{O}/\text{H}_2^{16}\text{O}$ ratios. The observations obtained from the full HIFI spectral survey of IRC+10216 necessarily entail relatively short integration times at any given frequency within the large HIFI frequency range. In this paper, we report results of significantly improved sensitivity obtained from deep observations that target the $1_{10} - 1_{01}$ transitions of H_2^{17}O at 552.021 GHz and of H_2^{18}O at 547.676 GHz. The H_2^{16}O $1_{10} - 1_{01}$ line at 556.936 GHz had been observed previously by *Herschel*/HIFI but – to ensure a meaningful comparison of lines measured toward a variable star – was reobserved at the same time as the H_2^{17}O and H_2^{18}O transitions. In §2 below, we discuss the new observations and the methods used to reduce the data. The results are presented in §3 and discussed in §4.

2. Observations and data reduction

The observations of IRC+10216 were carried out on 2011 May 18 in the Open Time program OT2_dneufeld_6. We used HIFI in dual beam switch (DBS) mode to target the $1_{10} - 1_{01}$ rotational transitions of H_2^{16}O , H_2^{17}O , and H_2^{18}O in mixer band 1a. The details of each observation are given in Table 1. The telescope beam, of diameter $\sim 38''$ (HPBW), was centered on IRC+10216 at coordinates $\alpha = 9\text{h } 47\text{m } 57.41\text{s}$, $\delta = +13^\circ 16' 43.6''$ (J2000), and the reference positions were located at offsets of $3'$ on either side of the source. The wide band spectrometer (WBS) was used to obtain a spectral resolution of 1.1 MHz, corresponding to a Doppler velocity ~ 0.6 km/s at the frequency of the observed transitions. The data were processed using the *Herschel* Interactive Processing Environment (HIPE; Ott 2010), version 9.0.0, providing fully calibrated spectra with the intensities expressed as antenna temperature and the frequencies in the frame of the Local Standard of Rest (LSR). Given a *Herschel* aperture efficiency of 0.68 (Roelfsema et al. 2012), the ratio of antenna temperature to flux is 2.1 mK/Jy for an unresolved source at the center of the beam.

For each spectral line, we used three separate local oscillator (LO) frequencies, evenly spaced by a small offset, to facilitate sideband deconvolution. The standard deconvolution tool is optimized for spectral scans in which the redundancy is 4 or greater and the LO

observed line profiles, which provide no evidence for any radial dependence in the relative abundances of the various isotopologues.

spacings are slightly uneven; if the redundancy is less than 4, the standard method fails to remove small artifacts. We therefore used a maximum-entropy deconvolution method to decompose the double sideband spectra into a pair of single-sideband spectra. Because the entropy of the artifacts mentioned above is small, this method allows a reliable solution to be determined by minimizing χ^2 while keeping the so-called “gain entropy” high. We were able to confirm the results of this method by comparing them with spectra derived by manually separating the strongest LSB and USB lines.

After performing the sideband deconvolution as described above, we found the resultant spectra obtained for the horizontal and vertical polarizations to be very similar in their appearance and noise characteristics. We therefore coaveraged the two orthogonal polarizations, and – to improve the signal-to-noise ratio – then rebinned the spectra to a velocity-resolution of 3 km/s.

3. Results

Figures 1 and 2 show the spectra targeting H_2^{17}O and H_2^{18}O obtained from the data reduction procedure described in §2 above. The underlying noise ~ 1 mK (r.m.s. in the smoothed spectra) is consistent with the predictions of the HSPOT time estimator, but the spectra are clearly characterized by a high density of emission features. For lines with peak antenna temperatures exceeding ~ 10 mK (~ 5 Jy), plausible identifications were readily obtained from standard catalogs² and are marked in Figures 1 and 2; here the width of each mark indicates the uncertainty in the line frequency (or, in the case of AlCl, the frequency spread of the hyperfine components). However, for lines weaker than ~ 5 Jy, no plausible identification was obvious. Many of these weak unidentified lines are relatively narrow, implying expansion velocities ≤ 6 km/s and suggesting an origin close to the star. In this respect, the spectrum is rather similar to that obtained in the 345 GHz spectral survey of IRC+10216 carried out by Patel et al. (2011), which revealed a new population of weak, narrow, and mainly unidentified emission features that the authors attributed to uncatalogued transitions within vibrationally-excited states. Given the density of emission features in the spectra that we obtained, the incompleteness of current line catalogs unfortunately limits our ability (more so than the intrinsic signal-to-noise ratio) to identify very weak emissions from H_2^{17}O and H_2^{18}O unequivocally. (On the other hand, improvements in the limits derived below may be possible as line catalogs become more complete, allowing weak interlopers to

²The Cologne Database for Molecular Spectroscopy (CDMS; Müller et al. 2001, 2005), the JPL line list (Pickett et al. 1998), and Splatalogue (Remijan & Markwick-Kemper 2007)

be identified and their relative line strengths modeled.)

In Figures 3 and 4, we show the spectra targeting H_2^{17}O and H_2^{18}O (black histograms) on an expanded velocity scale, with vertical dotted lines indicating the velocity centroid (-26.5 km/s) and outflow velocity (14.5 km/s) inferred from observations of other spectral lines. For the H_2^{17}O transition (Figure 3), there is no evidence for excess emission at the LSR velocity of the source, although our sensitivity is clearly limited by unidentified emission features at nearby velocities. The magenta histogram in this figure shows the H_2^{16}O line scaled by a factor of $1/220$; this being the strongest feature that could be accommodated under the observed spectral profile, we adopt $1/220$ as an upper limit on the $\text{H}_2^{17}\text{O}/\text{H}_2^{16}\text{O}$ line ratio. We note here that the H_2^{16}O line profile is considerably broader than the narrow unidentified emission features discussed above; its breadth is typical of other transitions within the ground vibrational states of circumstellar molecules, and is consistent with the predictions of excitation models for the H_2^{16}O $1_{10} - 1_{01}$ line (e.g. González-Alfonso, Neufeld, & Melnick 2007).

For the H_2^{18}O spectrum (Figure 4), a feature is clearly apparent close to the expected frequency of the H_2^{18}O transition, with an integrated antenna temperature ~ 71 mK km/s that exceeds our upper limit on the H_2^{17}O line. Given the $^{17}\text{O}/^{18}\text{O}$ isotopic ratio ~ 1.5 in IRC+10216 (Kahane et al. 1992), it would be surprising to find a $1_{10} - 1_{01}$ line of H_2^{18}O that was *stronger* than that of H_2^{17}O . A careful search of available line catalogs revealed an interloper transition of vibrationally-excited HNC, the $\nu_2 = 1f$ $J = 6 - 5$ line, which has a frequency offset (relative to H_2^{17}O $1_{10} - 1_{01}$) of only ~ -6 MHz, corresponding to a velocity offset $\sim +3$ km/s. Based upon a model for the excitation of HNC, constrained by *Herschel* observations of the ground vibrational state (Daniel et al. 2012) along with ALMA observations of transitions of lower frequency within the $\nu_2 = 1$ state (Daniel et al. in preparation), we expect a velocity integrated antenna temperature of 62 mK km/s for this HNC transition (with the line strength and profile shown in red). After subtraction of the expected HNC emission, the observed spectrum (blue) shows no clear evidence for any residual that could be attributed to H_2^{18}O .

4. Discussion

Because our sensitivity to H_2^{18}O is limited by the precision with which we can model the interloper HNC $\nu_2 = 1f$ $J = 6 - 5$ line, and given the inferred *photospheric* isotopic ratio of $^{17}\text{O}/^{18}\text{O} \sim 1.5$, we will focus on the H_2^{17}O line intensity limit as a constraint on the extent of any isotope-selective enhancement in the minor isotologues of water. Using the model of González-Alfonso et al. (2007) for the excitation of water in IRC+10216, we found

that the observed line intensity limit, $\text{H}_2^{17}\text{O } 1_{10} - 1_{01} / \text{H}_2^{16}\text{O } 1_{10} - 1_{01} < 1/220$ implies an abundance ratio limit $\text{H}_2^{17}\text{O} / \text{H}_2^{16}\text{O} < 1/470$ (the latter being smaller than the former on account of optical-depth effects for H_2^{16}O). Comparing this with the isotopic $^{17}\text{O}/^{16}\text{O}$ ratio of $1/840$, we can place a conservative upper limit of 1.8 on the factor, f_e , by which the minor isotopologues are enhanced.

This limit on f_e places a strong constraint on any model in which the photodissociation of CO is the source of atomic oxygen to form water in IRC+10216. For example, were ^{13}C the primary source of ^{16}O and C^{17}O that of ^{17}O , then the expected enhancement factor (Neufeld et al. 2011a) would be $f_e \sim ^{12}\text{C}/^{13}\text{C} = 45$ (Cernicharo et al. 2000). Such a large enhancement factor is entirely inconsistent with the data reported here, and would argue against the clumpy photodissociation model and in favor of the alternative model proposed by Cherchneff (2011, 2012). However, as noted by Neufeld et al. (2011a), this large predicted enhancement might be decreased if photodissociation of ^{12}CO or SiO contributed significantly to ^{16}O production. Moreover, the photodissociation of ^{12}CO in vibrationally-excited states that are populated close to the star might further reduce the enhancement factor. A proper account of these effects will require an extensive theoretical study, beyond the scope of this *Letter*, in which the clumpy photodissociation model is investigated fully with detailed treatments of radiative transfer and of the photodissociation of vibrationally-excited CO.

In any such model, photodissociation of $^{12}\text{C}^{16}\text{O}$ would necessarily have to be the primary source of ^{16}O . Barring any gas-phase fractionation effects, which would to have been extremely minor at the high gas temperatures in the inner envelope, the observed upper limit on $\text{H}_2^{16}\text{O}/\text{H}_2^{17}\text{O}$ would imply that ^{16}O must be produced at least 470 times as fast (per unit volume) as ^{17}O . Since the latter is produced by photodissociation of $^{12}\text{C}^{17}\text{O}$, the photodissociation of $^{12}\text{C}^{16}\text{O}$ is the only photodissociation process that could possibly provide ^{16}O at a sufficient rate; no other oxygen-bearing molecule is abundant enough to yield the required ^{16}O production rate as a result of its photodissociation.³

HIFI has been designed and built by a consortium of institutes and university departments from across Europe, Canada and the United States under the leadership of SRON Netherlands Institute for Space Research, Groningen, The Netherlands and with major contributions from Germany, France and the US. Consortium members are: Canada: CSA, U. Waterloo; France: CESR, LAB, LERMA, IRAM; Germany: KOSMA, MPIfR, MPS;

³Although SiO has an unshielded photodissociation rate that is ~ 6 times as large as that of $^{12}\text{C}^{17}\text{O}$ (van Dishoeck, Jonkeid & van Hemert 2006; Visser, van Dishoeck & Black 2009), its abundance is only $\sim \text{few} \times 10^{-7}$ relative to H_2 (Decin et al. 2010b), i.e. even less than that of $^{12}\text{C}^{17}\text{O}$.

Ireland, NUI Maynooth; Italy: ASI, IFSI-INAF, Osservatorio Astrofisico di Arcetri- INAF; Netherlands: SRON, TUD; Poland: CAMK, CBK; Spain: Observatorio Astronómico Nacional (IGN), Centro de Astrobiología (CSIC-INTA). Sweden: Chalmers University of Technology - MC2, RSS & GARD; Onsala Space Observatory; Swedish National Space Board, Stockholm University - Stockholm Observatory; Switzerland: ETH Zurich, FHNW; USA: Caltech, JPL, NHSC.

This research was performed, in part, through a JPL contract funded by the National Aeronautics and Space Administration. E.G-A is a Research Associate at the Harvard-Smithsonian Center for Astrophysics, and thanks the Spanish Ministerio de Ciencia e Innovación for support under project AYA2010-21697-C05-01. R. Sz. and M. Sch. acknowledge support from Polish NCN grant no. 203 581040.

REFERENCES

- Agúndez, M., & Cernicharo, J. 2006, *ApJ*, 650, 374
- Agúndez, M., Cernicharo, J., & Guélin, M. 2010, *ApJ*, 724, L133
- Cernicharo, J., Guélin, M., & Kahane, C. 2000, *A&AS*, 142, 181
- Cherchneff, I. 2011, *A&A*, 526, L11
- Cherchneff, I. 2012, *A&A*, 545, A12
- Daniel, F., Agúndez, M., Cernicharo, J., et al. 2012, *A&A*, 542, A37
- Decin, L., et al. 2010a, *Nature*, 467, 64
- Decin, L., Cernicharo, J., Barlow, M. J., et al. 2010b, *A&A*, 518, L143
- de Graauw, T., et al. 2010, *A&A*, 518, L6
- Ford, K. E., & Neufeld, D. A. 2001, *ApJ*, 557, L113
- González-Alfonso, E., Neufeld, D. A., & Melnick, G. J. 2007, *ApJ*, 669, 412
- Kahane, C., Cernicharo, J., Gomez-Gonzalez, J., & Guélin, M. 1992, *A&A*, 256, 235
- Lyons, J. R., & Young, E. D. 2005, *Nature*, 435, 317
- Melnick, G. J., Neufeld, D. A., Ford, K. E. S., Hollenbach, D. J., & Ashby, M. L. N. 2001, *Nature*, 412, 160

- Müller, H. S. P., Thorwirth, S., Roth, D. A., & Winnewisser, G. 2001, *A&A*, 370, L49
- Müller, H. S. P., Schlöder, F., Stutzki, J., & Winnewisser, G. 2005, *Journal of Molecular Structure*, 742, 215
- Neufeld, D. A., González-Alfonso, E., Melnick, G. J., et al. 2011, *ApJ*, 727, L28
- Neufeld, D. A., González-Alfonso, E., Melnick, G., et al. 2011, *ApJ*, 727, L29
- Ott, S. 2010, *Astronomical Data Analysis Software and Systems XIX*, 434, 139
- Patel, N. A., Young, K. H., Gottlieb, C. A., et al. 2011, *ApJS*, 193, 17
- Pickett, H. M., Poynter, R. L., Cohen, E. A., et al. 1998, *J. Quant. Spec. Radiat. Transf.*, 60, 883
- Pilbratt, G. L., et al. 2010, *A&A*, 518, L1
- Remijan, A. J., Markwick-Kemper, A., & ALMA Working Group on Spectral Line Frequencies 2007, *Bulletin of the American Astronomical Society*, 39, #132.11
- Roelfsema, P. R., Helmich, F. P., Teyssier, D., et al. 2012, *A&A*, 537, A17
- van Dishoeck, E. F., Jonkheid, B., & van Hemert, M. C. 2006, *Faraday Discussions*, 133, 231
- Visser, R., van Dishoeck, E. F., & Black, J. H. 2009, *A&A*, 503, 323
- Willacy, K. 2004, *ApJ*, 600, L87

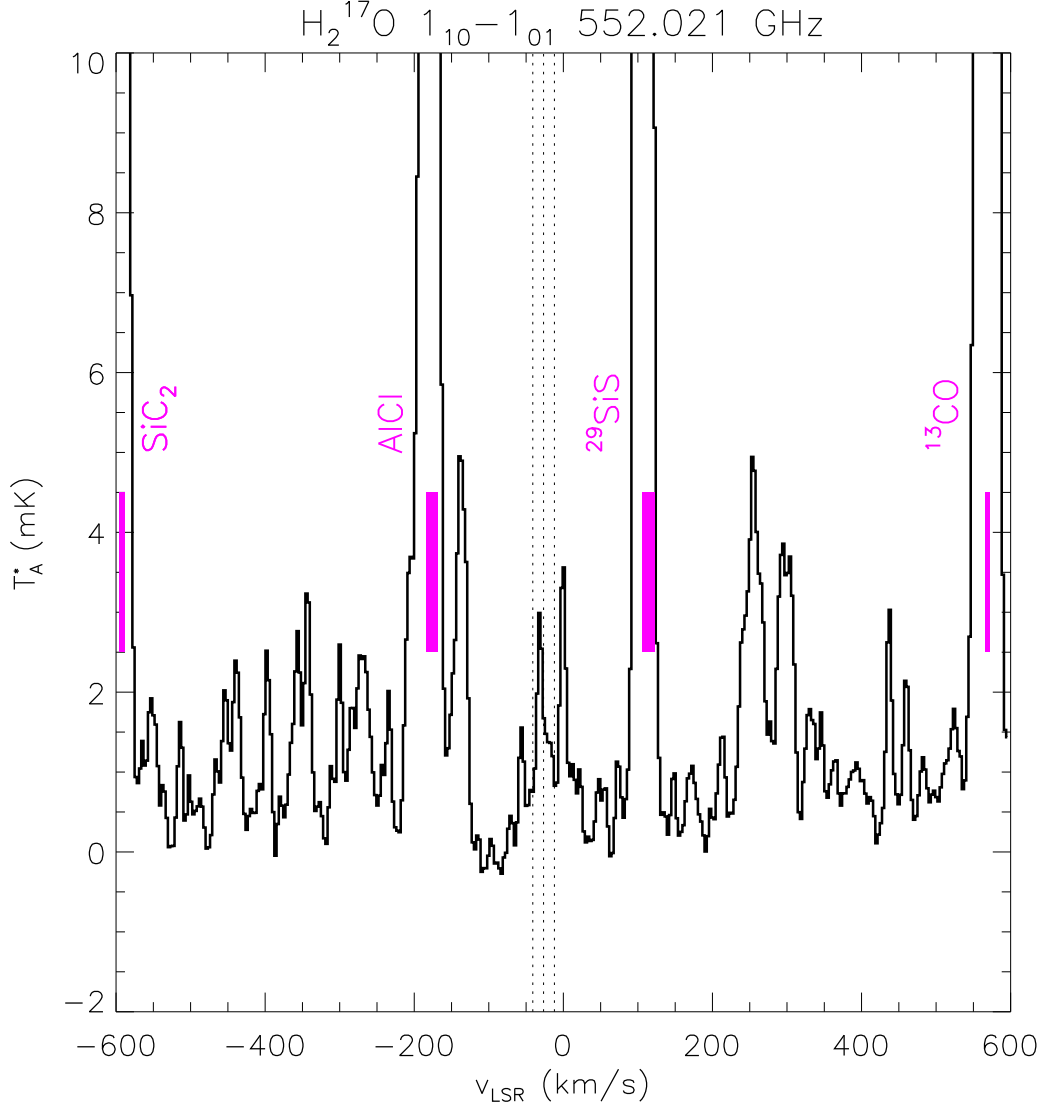


Fig. 1.— Spectrum targeting the $1_{10} - 1_{01}$ transition of H_2^{17}O in IRC+10216. The LSR velocity scale is for the 552.021 GHz rest frequency of that transition. Vertical dotted lines indicate the velocity centroid (-26.5 km/s) and outflow velocity (14.5 km/s) determined from observations of other lines. Purple marks indicate probable line identifications obtained from standard catalogues (see text), with the width of each mark indicating the uncertainty in the line frequency, or - in the case of AlCl - the frequency spread of the hyperfine components.

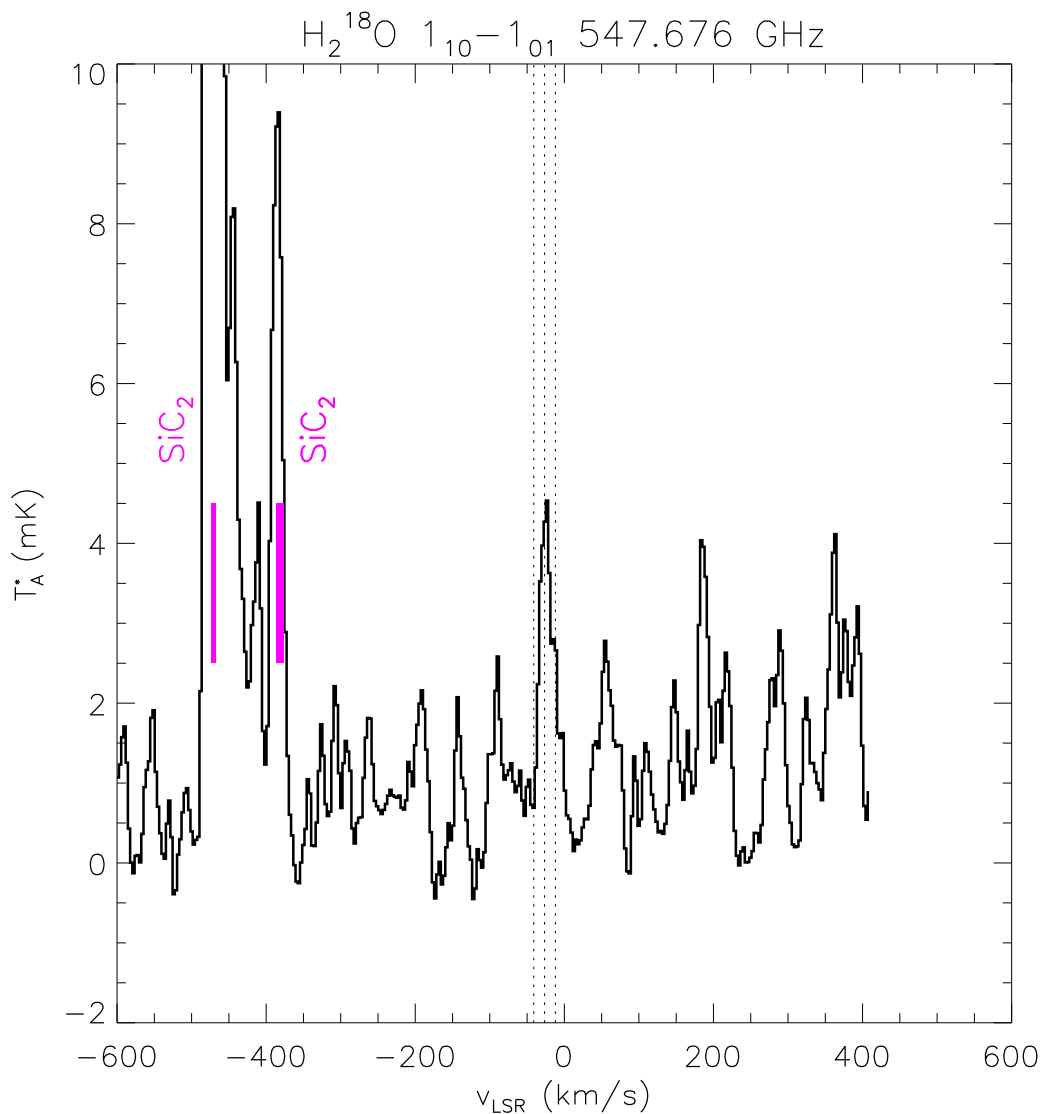


Fig. 2.— Spectrum targeting the $1_{10} - 1_{01}$ transition of H_2^{18}O in IRC+10216. The LSR velocity scale is for the 547.676 GHz rest frequency of that transition. Vertical dotted lines indicate the velocity centroid (-26.5 km/s) and outflow velocity (14.5 km/s) determined from observations of other lines. Purple marks indicate probable line identifications obtained from standard catalogues (see text), with the width of each mark indicating the uncertainty in the line frequency, or - in the case of AlCl - the frequency spread of the hyperfine components.

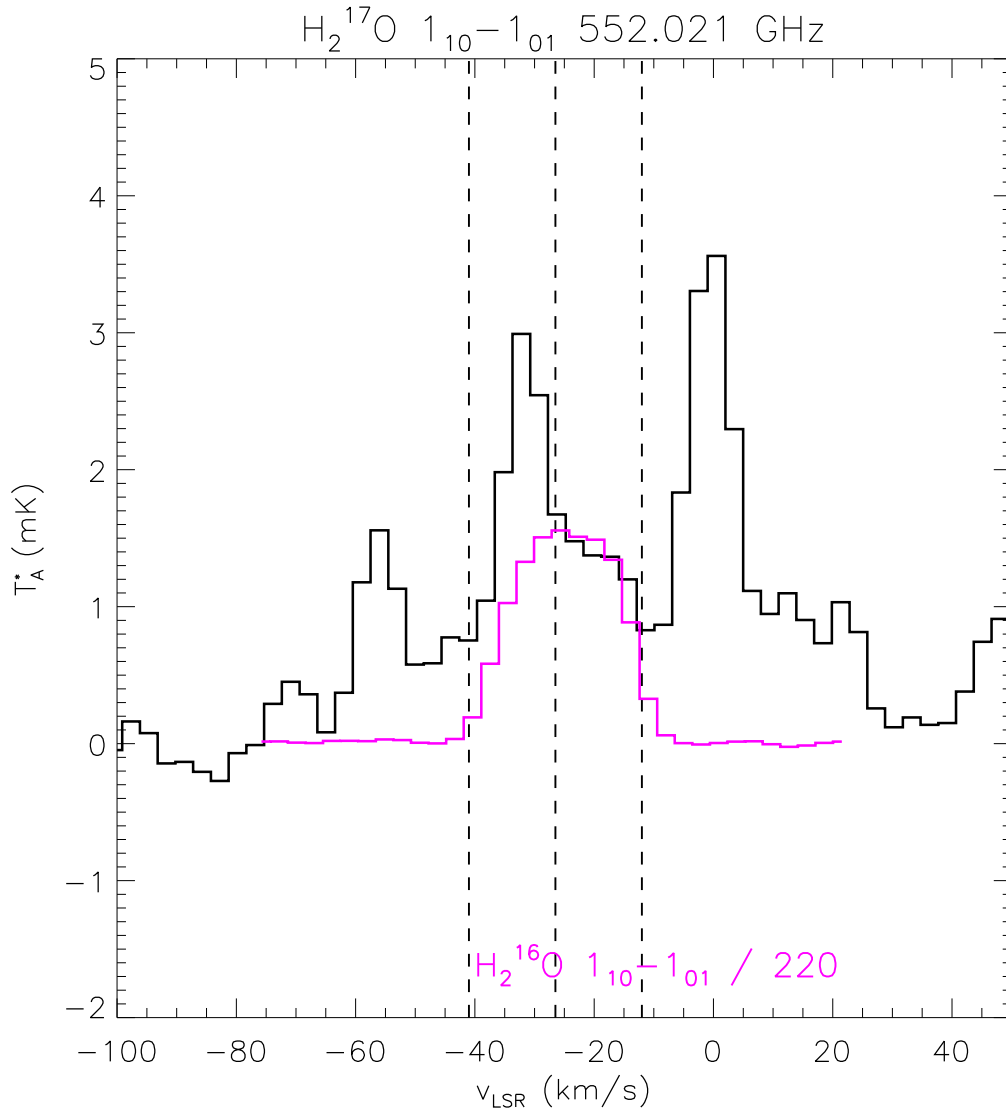


Fig. 3.— Same as Figure 1, but on an expanded velocity scale. Magenta histogram: H_2^{16}O $1_{10} - 1_{01}$ line scaled by a factor of 1/220.

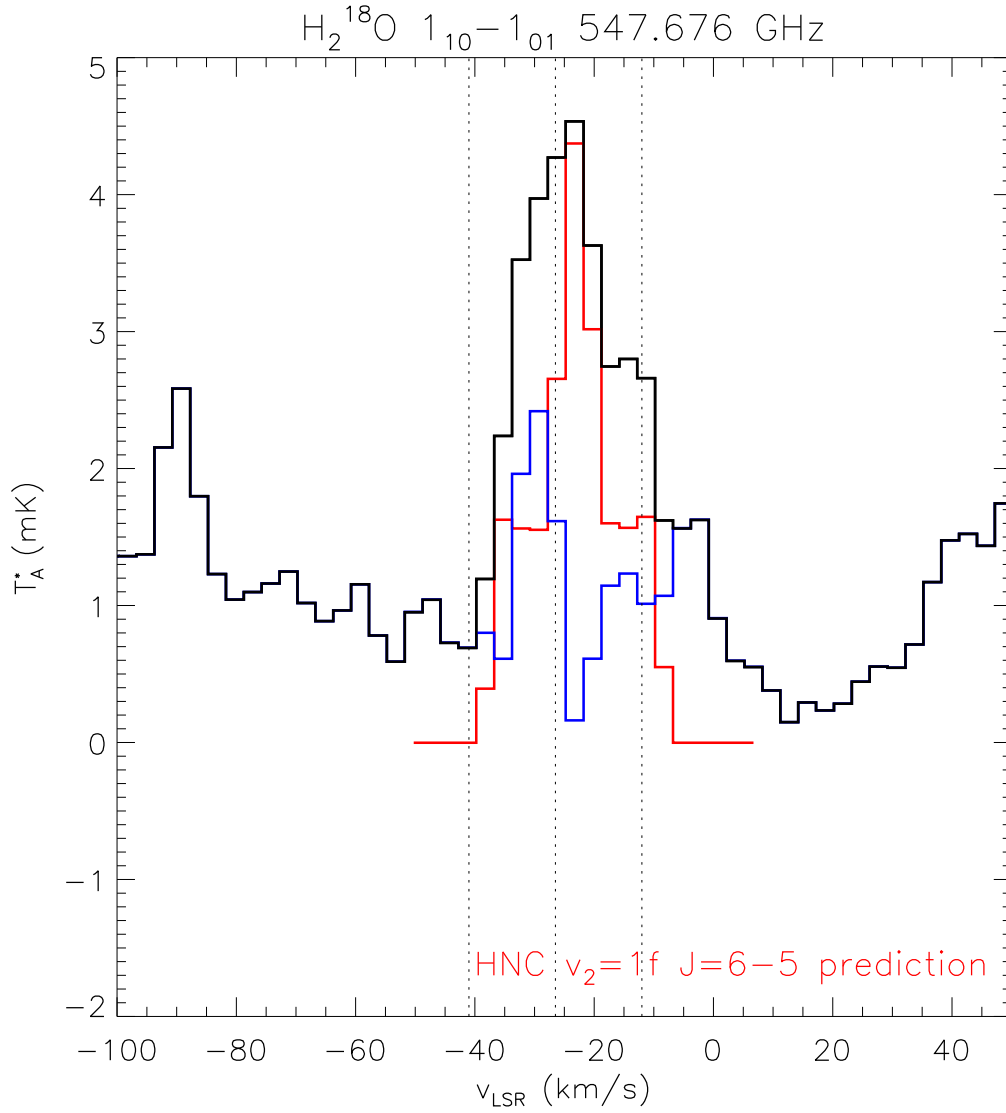


Fig. 4.— Same as Figure 2, but on an expanded velocity scale. Red histogram : prediction for the HNC $\nu_2 = 1f \ J = 6 - 5$ line. Blue histogram: data, after subtraction of the emission attributable to HNC $\nu_2 = 1f \ J = 6 - 5$.

Table 1. Observations of IRC+10216

Target transition	ν (GHz)	t_{obs}^a (s)	AOR #s
H ₂ ¹⁸ O 1 ₁₀ – 1 ₀₁	547.676	29701	1342246477–79
H ₂ ¹⁷ O 1 ₁₀ – 1 ₀₁	552.021	13104	1342246480–82
H ₂ ¹⁶ O 1 ₁₀ – 1 ₀₁	556.936	434	1342246483–85

^aTotal observing time for three LO settings